Information Content Analysis for Selection of Optimal JWST Observing Modes for Transiting Exoplanet Atmospheres

N.E. Batalha[1]

Department of Astronomy & Astrophysics, Pennsylvania State University, State College, PA 16802

neb149@psu.edu

and

M.R. Line [2]

Arizona State University, Tucson, AZ 85719

Received _____; accepted _____

[1]Center for Exoplanets and Habitable Worlds, Pennsylvania State University, State College, PA 16802

ABSTRACT

The James Webb Space Telescope is nearing its launch date of 2018, and will undoubtedly revolutionize our knowledge of exoplanet atmospheres. However, little has been done to identify which instruments and observing modes will be most useful for characterizing a diverse range of exoplanetary atmospheres. We use an information content based approach commonly used in the studies of Earth and Solar System atmospheres. We develop a scoring system based upon these information content methods to trace the instrumental and atmospheric model phase space in order to identify which observing modes are best suited for particular classes of planets. We find that for transmission and emission spectra, it is never beneficial to sacrifice wavelength coverage with multiple modes, over higher precision in a single mode. For transmission spectra, regardless of planet type (hot/cold, low/high C/O, low/high Fe/H), the best modes for constraining temperature profiles, C/O ratio and metalicity are: NIRISS SOSS+NIRSpec G395, NIRSpec G140+NIRSpec G395. For emission spectra of T_{eq} >1000 K planets, the best modes for constraining atmospheric parameters are NIRISS SOSS+NIRSpec G395, NIRSpec G235+MIRI LRS and, NIRISS SOSS+MIRI LRS. If the target's host star is dim enough such that the NIRSpec Prism can be used, then the combination of NIRISS SOSS+NIRSpec G395 can be substituted for the Prism. However, observations of emission spectra taken of T_{eq} <1000 K planets, must include MIRI LRS in order to constrain any atmospheric parameters.

Subject headings:

1. Introduction

For transmission spectroscopy alone, the James Webb Space Telescope (JWST) is equipped with eleven different observation modes across eight different wavelength ranges and six different resolutions. While there has been some work to identify what the limits of these modes will be, in terms of exoplanet characterization (Barstow et al. 2015a,b; Batalha et al. 2015; Greene et al. 2016), little work has been done to identify which instrument modes or combinations of modes will be most useful for characterizing a diverse range of exoplanetary atmospheres. The most rigorous way of accomplishing this is through atmospheric retrieval, which links atmospheric models to the data in a Bayesian framework (Line et al. 2012; Madhusudhan 2012).

For example, Barstow et al. (2015a) simulated an observation with NIRSpec Prism and MIRI LRS for four specific case studies: a hot Jupiter, a hot Neptune, GJ 1214 and Earth. For each observation they performed a full retrieval analysis to determine the prospects for identifying the true atmospheric state of the planet and assessed the possible effects of star spots and stitching on the results. Greene et al. (2016) also simulated the observations four specific planet archetypes (hot Jupiter, warm Neptune, warm sub-Neptune, cool Super-Earth) in three different combinations of modes: NIRISS only, NIRISS+NIRCAM, NIRISS+NIRCAM+MIRI. They concluded that spectra spanning 1-2.5μm will often provide good constraints on the atmospheric state but that in the case of cloudy or high mean molecular weight atmospheres a 1-11μm spectrum will be necessary. While both these studies offer insights into what kind of data we can hope to get from JWST, they do not simulate observations for a diverse instrument phase space for a wide variety of planet types because MCMC methods are cumbersome and slow. This, however, is necessary if we want to be able to optimize our science output with JWST.

To solve this problem, we use information content (IC) analysis, commonly used in

studies of Earth and Solar System atmospheres. With regards to Earth, Kuai et al. (2010) used IC analysis to determine the 20 best channels from each CO_2 spectral region for retrieving the most precise CO_2 abundance measurements taken with the Orbiting Carbon Observatory. Using the channels selected from their pipeline, they were able to achieve precision better than 0.1 ppm. Similarly, Saitoh et al. (2009) demonstrated that separately selecting a subset of the 15-μm CO_2 channels based on IC analysis, yielded the same precision on their retrieved results as the entire 15-μm band.

IC analysis has also been used with regards to exoplanets. Line et al. (2012) quantified the increase in information content that comes from an increase in signal to noise and resolution for an arbitrary wavelength range, 1-3 μm, and for a single planet case. Here we expand this analysis to look at planet archetypes ranging from T_{eq}=600-1800 K, C/O=0.55-1, Fe/H=1-100×Solar, across every possible combination of JWST transit spectroscopy modes. In doing so we answer the following questions:

1. Is there a combination of modes that will provide a higher precision of the retrieved model parameters?

2. And, does that combination of modes differ from transmission to emission? Or across different combinations of C/O ratio, metalicity, or temperature?

3. Is it better to sacrifice wavelength coverage across several different modes or to beat down the error in a single mode?

4. Is there a point where the addition of another mode results in the saturation of information content?

In §2 we explain the theory of IC analysis, in §3 we explain our transmission and emission forward models and in §4 we describe our JWST noise simulator. In §5, we look

at the results of the IC analysis and verify the results using a retrieval algorithm in §6. In §7 we discuss these results and end with concluding remarks in §8.

2. Information Content

In retrieval (Chahine 1968; Rodgers 1976; Twomey et al. 1977), the goal is to obtain the most likely set of model parameters given a set of observations. The model parameters, which define the atmospheric state, are just a vector, $\mathbf{x}$, of length n that usually is composed of mixing ratios, temperature, and any other atmospheric parameters pertinent to the model. The relationship between $\mathbf{x}$ and the observations is given by

$$\mathbf{y} = \mathbf{F}(\mathbf{x_a}) + \mathbf{K}(\mathbf{x} - \mathbf{x_a}) \tag{1}$$

where $\mathbf{F(x)}$ is the model and $\mathbf{x_a}$ is the initial guess of the true state (also known as the prior). $\mathbf{K}$ is an $m \times n$ Jacobian matrix given by

$$K_{ij} = \frac{\partial F_i(\mathbf{x})}{\partial x_j} \tag{2}$$

The Jacobian describes how sensitive the model is to slight perturbations in each state vector parameter at each wavelength position. F_i is the measurement in the i^{th} channel and x_j is the j^{th} state vector parameter.

For this analysis the parameters in the state vector, $\mathbf{x}$ are: $\mathbf{x} = [T, C/O, Fe/H, x\mathrm{R}_p]$. We use a two part model, described in §3 to compute the transmission ($Z_\lambda = (R_{p,\lambda}/R_*)^2$) or emission $Z_\lambda = (F_{p,\lambda}/F_*)$ spectrum. Because there is no analytic solution to compute the partial derivative in (2), we use a finite differencing method with 10% perturbations.

Therefore, (2) becomes a # of wave bins ×4 matrix:

$$\mathbf{K} = \begin{bmatrix} \frac{\partial Z_{\lambda_1}}{\partial C/O} & \frac{\partial Z_{\lambda_1}}{\partial Fe/H} & \frac{\partial Z_{\lambda_1}}{\partial T} & \frac{\partial Z_{\lambda_1}}{\partial xR_p} \\ \frac{\partial Z_{\lambda_2}}{\partial C/O} & \frac{\partial Z_{\lambda_2}}{\partial Fe/H} & \frac{\partial Z_{\lambda_2}}{\partial T} & \frac{\partial Z_{\lambda_2}}{\partial xR_p} \\ \vdots & \vdots & \vdots & \vdots \\ \frac{\partial Z_{\lambda_m}}{\partial C/O} & \frac{\partial Z_{\lambda_m}}{\partial Fe/H} & \frac{\partial Z_{\lambda_m}}{\partial T} & \frac{\partial Z_{\lambda_m}}{\partial xR_p} \end{bmatrix} \tag{3}$$

The information content, measured in bits, qualitatively describes how the state of knowledge (relative to the prior) has increased by making a measurement (Shannon & Weaver 1962; Line et al. 2012). It is computed as the reduction in entropy of the probability that an atmospheric state exists given a set of measurements:

$$H = entropy(P(\mathbf{x})) - entropy(P(\mathbf{x}|\mathbf{y})) \tag{4}$$

where

$$P(\mathbf{x}) \propto e^{-0.5(\mathbf{x}-\mathbf{x_a})^T \mathbf{S_a^{-1}} (\mathbf{x}-\mathbf{x_a})} \tag{5}$$

$$P(\mathbf{x}|\mathbf{y}) \propto e^{-0.5J(\mathbf{x})} \tag{6}$$

In (4) $\mathbf{S_a}$ is a $n \times n$ *a priori* covariance matrix, which defines the prior state of knowledge. $J(\mathbf{x})$ is the cost function which is given by:

$$J(\mathbf{x}) = (\mathbf{y} - \mathbf{K}\mathbf{x})^T {\mathbf{S_e}}^{-1} (\mathbf{y} - \mathbf{K}\mathbf{x}) + (\mathbf{x} - \mathbf{x_a})^T \mathbf{S_a^{-1}} (\mathbf{x} - \mathbf{x_a}) \tag{7}$$

The only piece not yet defined is $\mathbf{S_e}$, the $m \times m$ error covariance matrix, which defines the error on each measurement, in each channel. Therefore, the first segment in the cost function describes the data's contribution to the state of knowledge and the second describes the contribution from the prior.

Combining (3-5) with the knowledge that the entropy of a Gaussian distribution of width σ is proportional to $\ln \sigma$, we can rewrite (3) as:

$$H = \frac{1}{2} \ln(|\hat{\mathbf{S}}^{-1} \mathbf{S_a}|) \tag{8}$$

and

$$\hat{\mathbf{S}} = (\mathbf{K^T S_e^{-1} K} + \mathbf{S_a^{-1}})^{-1} \tag{9}$$

$\hat{\mathbf{S}}$ is the mean covariance of the posterior probability distribution. It is an $n \times n$ diagonal matrix whose elements approximate the retrieved uncertainties on the state parameters. Intuitively, we can verify that 7 & 8 are correct. If the error is very small and the elements of $\mathbf{S_e}$ approach 0, the retrieved uncertainties will approximate $\hat{\mathbf{S}} \approx \mathbf{K^T S_e^{-1} K}$ and the information content, H will be high if the elements of the Jacobian are large.

It is helpful to think of this in the context of exoplanet characterization and JWST. If we were only interested in deciding between NIRISS, NIRCam and MIRI to maximize the total retrievable information (let's say: T, $x\mathrm{R}_p$, C/O, Fe/H), the goal would be to minimize the elements of $\hat{\mathbf{S}}$. Because there will likely be little prior knowledge on these parameters, $\mathbf{S_a}^{-1} << \mathbf{K^T S_e^{-1} K}$. The mode with identically the highest sensitivity to each of the state vector parameters ($\mathbf{K}$) and the lowest error ($\mathbf{S_e}$), will have the the lowest values of $\hat{\mathbf{S}}$. We can ignore the dependency of the *a priori* matrix by using identical priors to compute the information content for NIRISS, NIRCam and MIRI. The mode with the highest value for H will yield the most information of the atmospheric state.

3. Atmospheric Modeling & Computing the Jacobians

In order to compute the Jacobian, we must define the model, $\mathbf{F}(\mathbf{x})$ and a state around which to compute the partial derivatives. We use the well-known chemical equilibrium model, CEA, to compute the atmospheric mixing ratios and two separate forward models to compute either the emission spectra or the transmission spectra.

The transmission forward model is described in Line et al. (2013b), Swain et al. (2014), Kreidberg et al. (2014) and Greene et al. (2016). The emission forward model is originally

described in Line et al. (2013a) and updates were made to it in Diamond-Lowe et al. (2014). The molecular opacities used to compute the forward model spectra are described in Line et al. (2015).

In transmission, we assume 1-D isothermal temperature profiles at the equilibrium temperature and we assume that the mixing ratio profiles are constant with altitude. In total, there are 7 model parameters, four of which are included in the state vector (T, C/O, Fe/H, $x\mathrm{R}_p$) for the IC analysis. The other three are used to parametrize clouds and hazes. Our grey cloud is set by adding a cloud-top pressure (P_c = 1 mbar) below which transmittance is zero. Hazes are modeled using the approximation in Lecavelier Des Etangs et al. (2008), which is given by

$$\sigma = \sigma_0 \left(\frac{\lambda}{\lambda_0} \right)^{-\beta} \tag{10}$$

Here, σ_0 is the magnitude of the haze cross section relative to H_2 Rayleigh scattering at 0.4μm and β describes the slope of the haze. In emission, there are 7 model parameters, five of which are used to compute a double-grey analytic formula for the 1-D T-P profile Line et al. (2013a). We do not add in clouds to the emission spectra since their impact is expected to be less drastic than that of transmission (Fortney 2005).

For all initial state vectors, $\mathbf{x}$, we assume a planet radius of R=1.39 R_J and mass of M=0.59 M_J around WASP-62. WASP-62 was chosen because it was identified as a potential target for the JWST Early Release Science (Stevenson et al. 2016). We do not explore parameter space in planet radius and mass, because changes in radius and mass will affect the spectrum uniformly in wavelength space (Line et al. 2012). Therefore, exploring this parameter will not help to optimize mode selection. Changing the stellar type will affect the error profiles because of the different SED peaks. These effects will be minor compared to the effects that come from changing temperature, C/O, Fe/H, and cloud profiles. Therefore, we fix the stellar type as well.

We explore 7 temperatures ranging from T_{eq} = 600-2000 K, 2 C/O ratios ranging from 0.55-1 and two metalicities ranging from Fe/H=1-100×Solar. For transmission, we explore three different cloud profiles: no clouds, grey cloud, and haze. For emission we only explore cloud free models. For each of these 112 combinations of planet types, we compute a separate Jacobian. Figure 1 shows the Jacobian for different C/Os and metalicites at a single temperature, T=1800 K. Notice that each combination of C/O and Fe/H has very different Jacobians. This further proves the need for an IC analysis so that instrument mode selection can be optimized without making assumptions of the atmospheric composition of the planet *a priori*.

4. JWST Noise Models

The noise simulator consists of two different components. The first, called *Pandeia*, is based on Space Telescope Science Institutes Exposure Time Calculator and supports all officially-supported JWST observing modes. The second, called *PandExo*, uses *Pandeia*s outputs to compute observation simulations of all observatory supported time-series spectroscopy modes.

Pandeia is a hybrid simulator, which uses a three-dimensional, pixel-based approach to simulate detector images. It does not include the entire field of view of the instrument, optical field distortion, intra-pixel response variations, or effects of jitter and drift. However, it does include the most up-to-date estimates for background noise, PSFs, instrument throughputs and optical paths, saturation levels, ramp noise, correlated noise, flat field errors and data extraction. Its final product is a 1D (wavelength) and 2D (wavelength + spatial) SNR simulation of a particular observation. Pandeia has already undergone rigorous testing against real images from the instrument teams and the source code is scheduled for release on January, 2017

PandExo requires a stellar SED model, stellar magnitude, planet spectrum (primary or secondary), the transit duration, fraction of time spent observing out of transit versus in transit, the desired exposure level and all the necessary instrument details (instrument, grism, filter, subarray). Then it calls *Pandeia* to create a 1D observation simulation of the out-of-transit (stellar SED) and the in-transit observation (stellar SED + planet model). Therefore, it does not model a full light curve with ingress and egress and does not account for any time-varying noise (i.e. stellar noise, jitter, drift). Its final product is a 1D planet spectrum with the associated error bars, which includes all the noise sources listed in §4.1.The error bars are used to create the error covariance matrices, $\mathbf{S_e}$ in (7).

5. IC Analysis Results

Not counting modes with overlapping wavelength space, there are approximately 8!∼40,320 combinations of modes on board JWST for exoplanet spectroscopy alone. In order to narrow down these combinations, we first focus on only two mode comparisons in transmission, followed by emission. To begin with, all noise simulations are computed for a single transit, unless otherwise specified.

Because it is not feasible to display 112 different maps of information content, we pick two representing planet types to display our results in figure form: T = 1800 K (Figure 2) and T = 600 K (Figure 3). The IC maps can be easily interpreted by finding the combination of modes in which, regardless of C/O or Fe/H, give the highest information content (i.e. common dark regions in all all four panels). We separate the maps by temperature because we assume it is the only reliable information that the observer will have *a priori* to base their observation off of.

Our predictions for the good combinations of modes and the worst combinations of

modes for transmission spectra are summarized in Table 1. The same for emission is summarized in Table 2. Note again that we did not explore the effect of clouds for emission spectra.

In short, for transmission, the combination of NIRISS and NIRSpec G395M/H yields the highest information content regardless of temperature, C/O and Fe/H. For emission, cooler planets with $T_{eq} < 1000$ K only have high information content if they are observed with MIRI LRS. Planets with $T_{eq} > 1000$ K all have highest information content if observed with NIRISS+G395M/H, NIRISS+LRS or G235M/H+LRS. This answers the entirety of question #1 & 2 in §1.

If it were better to sacrifice wavelength coverage for higher precision in one mode (quesiton #3 §1), there would be high information content in the diagonal elements of Figures 2-3 because the diagonal elements represent two observations in one mode. In fact, there was *never* a case where two transits in a single mode resulted in higher information content than two transits spread over two separate modes.

Lastly (question #4), is it possible to increase the information content of our two mode comparisons by adding more modes to the mix? Figure 8 shows, starting with NIRSpec G140M/H, the information content as a function of the addition of an instrument mode. The shaded regions in the figure show that there are spikes in information content with the addition of NIRISS and NIRSpec G395M/H (as expected). The addition of MIRI LRS adds a very slight (less than 1 bit) increase in information content. Because the addition of other modes do not sufficiently increase the information content, we conclude that there is a saturation of information content and that there is a such thing as "too many modes".

6. Verification of IC Analysis Results

Because IC analysis is not widely used in exoplanet science, we use the retrieval algorithm, *PyMultiNest*, which is paired with the well-tested retrieval code, CHIMERA, described in Line et al. (2013a). In order to test the efficacy of our IC analysis, we compare the retrieved results for our prediction of a "good combination" of modes against the retrieved results for our prediction of a "poor combination" of modes.

Figure 4 shows the results for the case of T = 1800 K in transmission. Here, our prediction for a "good" combination, NIRISS+NIRSpec G395M/H contains 9.2 bits of information. We compare this against an observation of NIRISS+NIRSpec G235M/H, which has 7.7 bits of information. For reference, the mode with the lowest value for information content is NIRCam F444+NIRCam F444, which has 5.5 bits of information. The posterior predictive histograms for temperature, C/O, and Fe/H are all more tightly constrained with the good combination. This suggests that just 2 bits of information does make a different in the retrieved results.

Figure 5 shows the results for the case of T = 600 K in emission. Here, our prediction for a "good" combination is NIRCam F444+LRS has 1.2 bits of information. We compare this to an observation of NIRSpec G140M/H+NIRCam F444, which has 0.293 bits of information. Here the posterior predictive histograms for temperature, C/O and Fe/H are also more tightly constrained with our prediction for the good combination of modes. A sophisticated retrieval algorithm proves the efficacy of our relatively simple IC analysis.

7. Discussion

7.1. Why NIRISS + G395M/H?

Table 1 shows that for in transmission, regardless of temperature, C/O, Fe/H or cloud properties, a combination of NIRISS+NIRSpec G395M/H yields the highest information content. It seems counter-intuitive that this combination of modes would be consistent accross so many different kinds of planet types.

However, intuitively, this makes sense because the combination of the two give relatively high resolution spanning 1-5 μm, wavelength coverage than other combinations. Mathematically, this makes sense because these wavelength regions are the locations of the spectrum with the highest rate of change with respect to the state vector parameters (the elements of the Jacobian are the highest). And physically, this makes sense because short of 2.5μm there are prominent absorption features of H_2O, CH_4 and between 4-5μm there is a precarious CO feature, whose presence/absence can be used to constrain C/O.

Because the high information content is a result of the wavelength region and not the error covariance, the observer could swap out the combination of NIRISS+G395M/H for the NIRSpec Prism. The NIRSpec Prism was not explored in this paper because it has a very high saturation limit (J$\sim$ 10.5). Therefore, the best JWST targets will saturate the NIRSpec Prism. We conclude that if the target is dim enough, it can be observed with the Prism instead of NIRISS and G395M/H. The observer would only be sacrificing lower resolution.

7.2. Effect of Increasing # of Transits

As previously mentioned, all of the calculations of the error covariance matrices were done for a single transit. This begs the question of whether or not higher precision (more transits) in any of the modes we explored would have altered our results

Looking at Figure 2, one can imagine that there is a third dimensions to this 2D image: the error achieved on your spectrum. To illustrate what this third dimension looks like, we show every single combination of two mode instrument combination (i.e. every single square in Figure 2 is transformed to function of IC versus error on spectrum). Additionally, we've only given a non-black color to our prediction for the best combination of modes in Table 1. This makes it simple to see that no matter what the error on the spectrum is, our prediction for a good combination of modes will always yield higher information content regardless of how small precise the measurement is.

8. Conclusion

Although IC analysis has not been used for channel selection in exoplanetary atmospheres, we conclude that it is an effective method for selecting JWST observing modes. We find that in transmission the combination of modes that gives the highest information content regardless of temperature, C/O, Fe/H and cloud assumptions is: NIRISS SOSS+NIRSpec G395M/H and NIRSpec G140M/H+NIRSpec G395M/H.

In emission, our prediction for a good combination of modes is dependent on temperature. Cool planets $T_{eq} < 1000$ do not have enough thermal emission in the near-IR to yield high information content observations. Therefore, anything less than $T_{eq} < 1000$ should only be be observed with MIRI LRS. For hotter planets $T_{eq} > 1000$, which do have flux in the near-IR, the following modes yield observations with high information content:

NIRISS SOSS+NIRSpec G395M/H, NIRISS SOSS+LRS, NIRSpec G235M/H+MIRI LRS.

We have also shown that it is not better to sacrifice wavelength coverage for more precise measurements over a small wavelength region, unless the planet is cool and being observed in emission.

All of these conclusions have been verified with a sophisticated retrieval method.

Lastly, observers are cautioned that selecting too many modes might result in a saturation in information content. In other words, for some observations the addition of more modes will not yield a higher degree of knowledge of the true atmospheric state. If this is the case, the observer should instead allocate its JWST time on another target or more precise measurements in the modes that do yield high information.

REFERENCES

Barstow, J. K., Aigrain, S., Irwin, P. G. J., et al. 2015, MNRAS, 451, 1306, (2015a)

Barstow, J.K., Bowles, N.E., Aigrain, S., et al. (2015), Experimental Astronomy, 40, 545B, (2015b)

Batalha, N., Kalirai, J., Lunine, J., Clampin, M., & Lindler, D. 2015, arXiv:1507.02655

Beichman, C., Benneke, B., Knutson, H., et al. 2014, PASP, 126, 1134

Chahine, M. T. 1968, JOSA (1917-1983), 58, 1634

Diamond-Lowe, H., Stevenson, K. B., Bean, J. L.,et al. 2014, ApJ, 796, 66

Fortney, J. J. 2005, MNRAS, 364, 649

Greene, T., Line, M., Montero, C., et al. 2016, ApJ, 817, 17G

Kuai, L., Natraj, V., Shia, R.L., et al., 2010, Journal of Quantitative Spectroscopy and Radiative Transfer, 11,9

Kreidberg, L., Bean, J. L.,Desert, J.-M., et al. 2014, ApJ, 793,LL27

Lecavelier Des Etangs, A., Pont, F., Vidal-Madjar, A., & Sing, D. 2008, A&A, 481, L83

Line, M. R., Zhang, X., Vasisht, G., et al., 2012, ApJ,749, 93L

Line, M. R., Wolf, A. S., Zhang, X., et al., 2013, ApJ,775, 137 (2013a)

Line, M. R., Knutson, H., Deming, D., Wilkins, A., Desert, J.M. 2013, ApJ, 778, 183 (2013b)

Line, M. R., Knutson, H., Wolf, A. S., & Yung, Y. L. 2014, ApJ,783, 70

Line, M. R., Teske, J., Burningham, B., Fortney, J. J., Marley, M. S. 2015, ApJ, 807, 183

Madhusudhan, N.,2012, ApJ, 758, 36

Rodgers, C.D. Reviews of Geophysics and Space Physics, 14, 609

Saitoh N, Imasu R, Ota Y, Niwa Y., J. Geophys. Res.114,D17

Shannon, C.E., & Weaver, W., A Mathematical Theory of Communication, Univ. of Illinois Press, 1962

Stevenson, Kevin B., Lewis, Nikole K., Bean, Jacob L., et al., 2014, PASP, 128, 967

Swain, M. R., Line, M. R., & Deroo, P. 2014, ApJ, 784, 133

Twomey, S., Herman, B., Rabinoff, R. 1977, JAS, 34, 1085

This manuscript was prepared with the AAS LaTeX macros v5.2.

Table 1: Two Mode Comparison: Transmission Spectrum

Planet Temp	Cloud	Modes w/ highest IC	Modes w/ lowest IC
600	cloud free	NIRISS+G395M/H G140M/H+G395M/H NIRISS+F444	F444+F444
	grey cloud	NIRISS+G395M/H G140M/H+G395M/H NIRISS+F322W2	G140M/H+G140M/H F444+F444
	haze	NIRISS+G395M/H G140M/H+G395M/H	F444+F444
1000	cloud free	NIRISS+G395M/H G140M/H+G395M/H	F444+F444
	grey cloud	NIRISS+G395M/H G140M/H+G395M/H NIRISS+F322W2	F444+F444
	haze	NIRISS+G395M/H G140M/H+G395M/H	F444+F444
1400	cloud free	NIRISS+G395M/H G140M/H+G395M/H NIRISS+F444	F444+F444
	grey cloud	NIRISS+G395M/H G140M/H+G395M/H NIRISS+F322W2	F444+F444
	haze	NIRISS+G395M/H G140M/H+G395M/H	F444+F444
1800	cloud free	NIRISS+G395M/H G140M/H+G395M/H NIRISS+F444	F444+F444
	grey cloud	NIRISS+G395M/H G140M/H+G395M/H NIRISS+F322W2	G140M/H+G140M/H F444+F444
	haze	NIRISS+G395M/H G140M/H+G395M/H	F444+F444

Table 2: Two Mode Comparison: Emission Spectrum

Planet Temp	Cloud	Mode w/ highest IC	Mode w/ lowest IC
600	cloud free	LRS	everything w/o LRS
1000	cloud free	LRS	G140M/H+G140M/H
1400	cloud free	NIRISS+G395M/H NIRISS+LRS G235M/H+LRS	G140M/H+G140M/H
1800	cloud free	NIRISS+G395M/H NIRISS+LRS G235M/H+LRS	G140M/H+G140M/H F444+F444

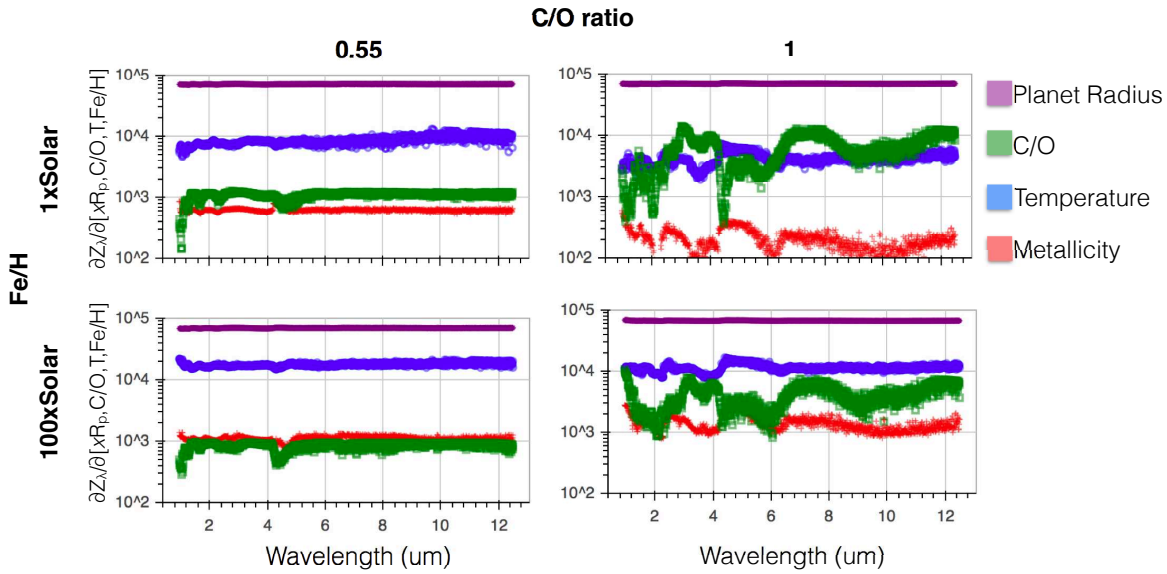

Fig. 1.— The elements of the Jacobian (Eqn. 2) for a transmission spectrum forward model. Partial derivatives were computed for a WASP-62 type star with a planet the size and mass of WASP-62 b. Atmosphere was computed assuming chemical equilibrium at $T_eq = 1800$ K with no clouds or hazes. Each panel represents a different combination of C/O and metalicity, as labeled.

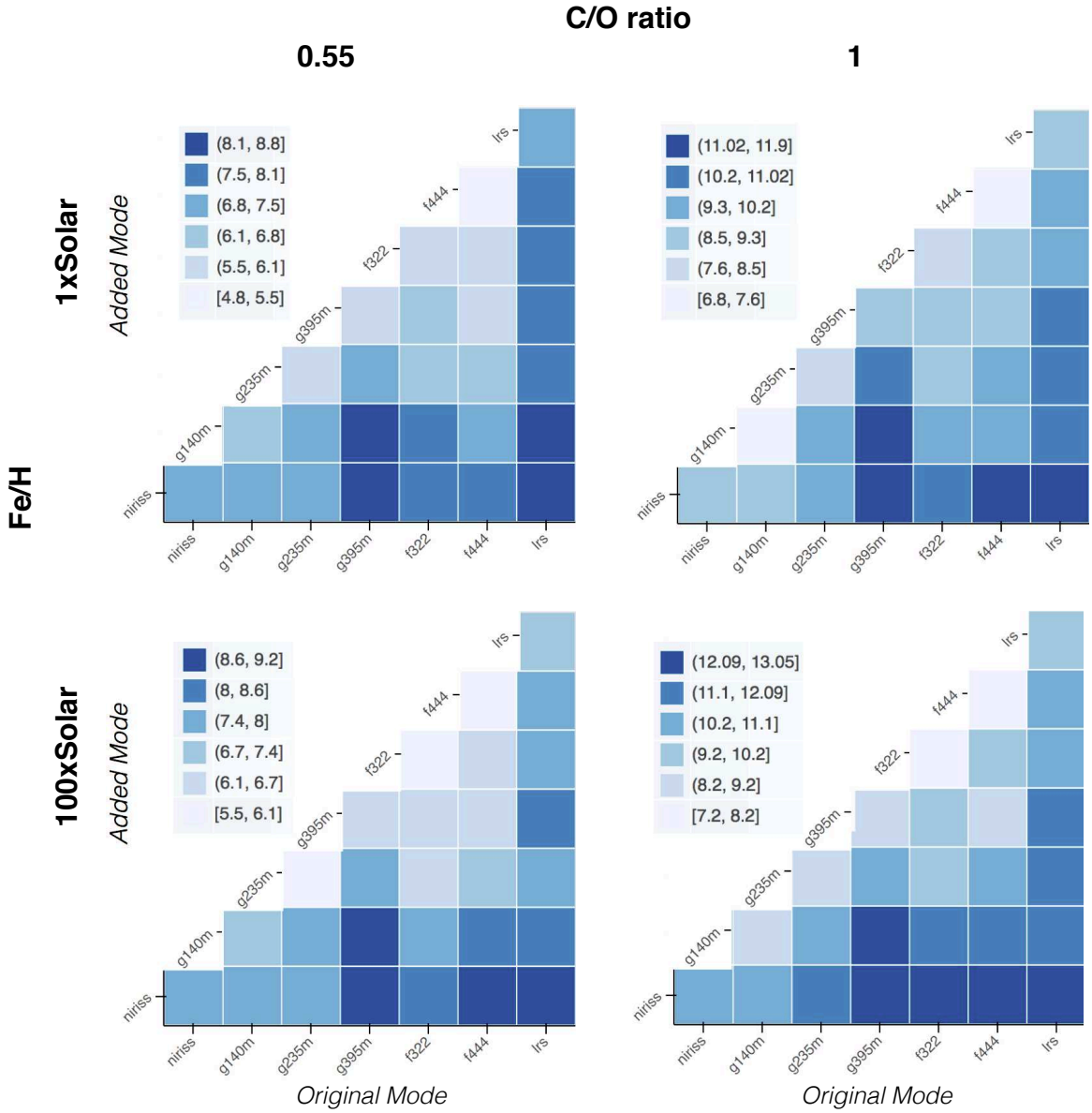

Fig. 2.— Information content maps for the same planet as shown in Figure 1. Rows are different metalicities and columns are different C/O ratios. Information content is measured in bits and the bins used for each map is shown next to each panel. Note that each panel has a different color scale. Diagonal elements are two transits in one mode. Observation modes which will maximize observers chances of obtaining the true atmospheric state appear as dark squares in all four panels.

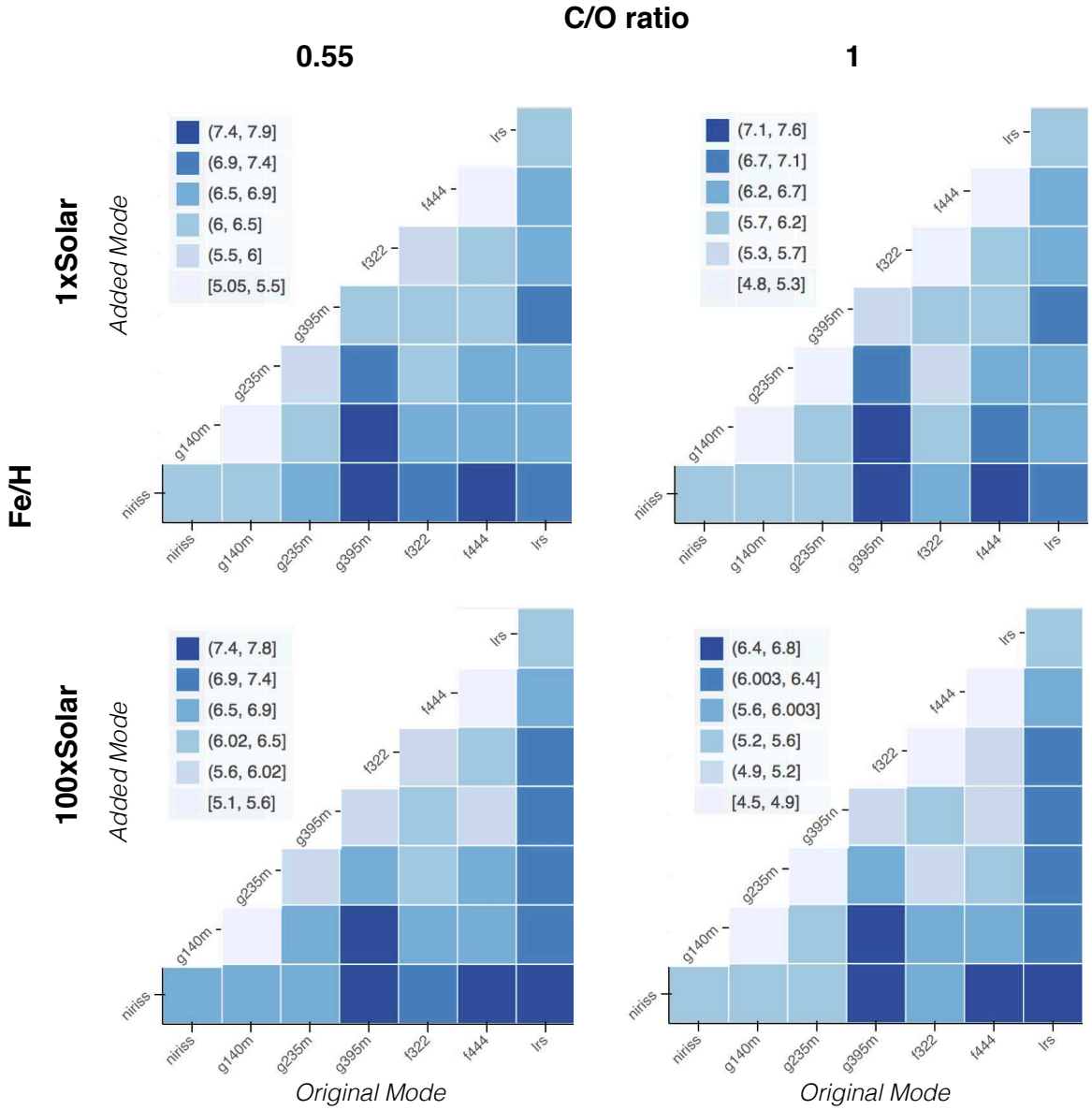

Fig. 3.— Information content maps for the same planet as shown in Figure 1 but with T_{eq} = 600 K. Rows are different metalicities and columns are different C/O ratios. Information content is measured in bits and the bins used for each map is shown next to each panel. Note that each panel has a different color scale. Diagonal elements are two transits in one mode. Observation modes which will maximize observers chances of obtaining the true atmospheric state appear as dark squares in all four panels.

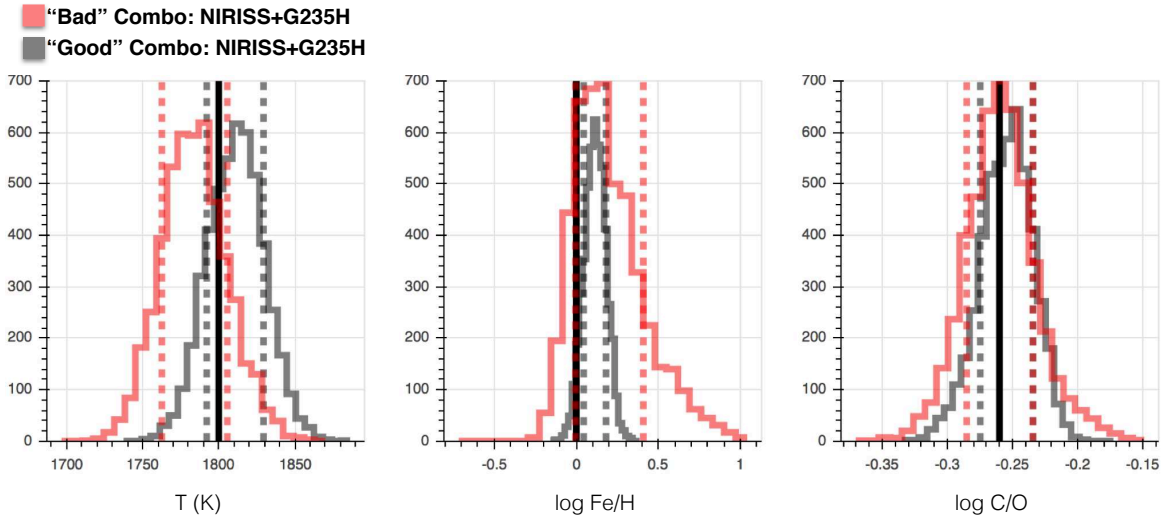

Fig. 4.— Retrieved quantities for transmission observations of the same WASP-62b system with T_{eq} = 1800 K (Figure 1). Posterior predictive histograms for the retrieved results are color coded by our prediction for a "good" combination of modes (black:NIRISS + NIRSpec G395M/H) versus our prediction for a "not-so-good" combination of modes (red:NIRISS + NIRSpec G235M/H). Opaque black line indicates true value.

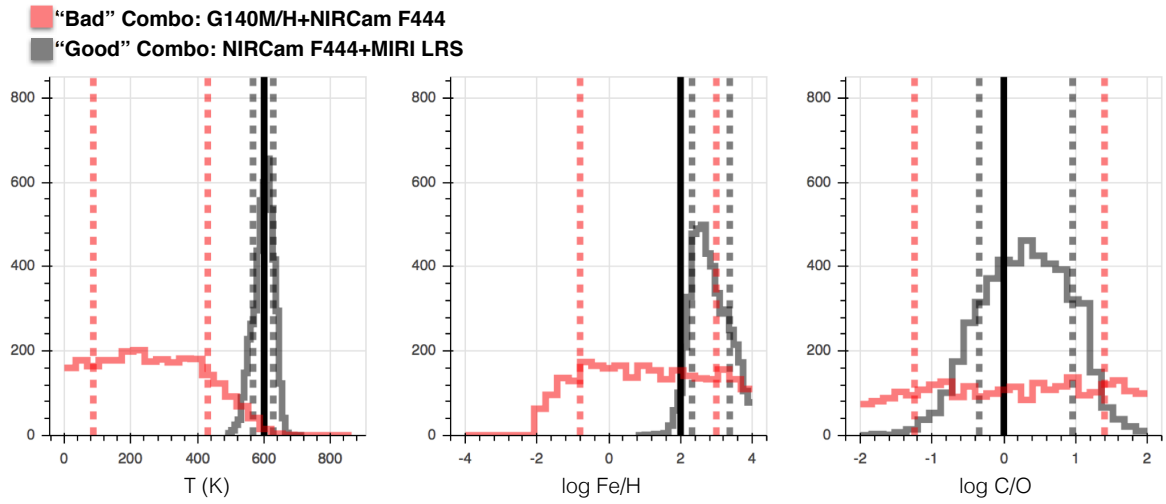

Fig. 5.— Retrieved quantities for emission observations of the same WASP-62b system with T_{eq} = 600 K (Figure 1). Posterior predictive histograms for the retrieved results are color coded by our prediction for a "good" combination of modes (black:NIRCam F444 + MIRI LRS) versus our prediction for a "not-so-good" combination of modes (red:G140M/H + NIRCam F444). Opaque black line indicates true value.

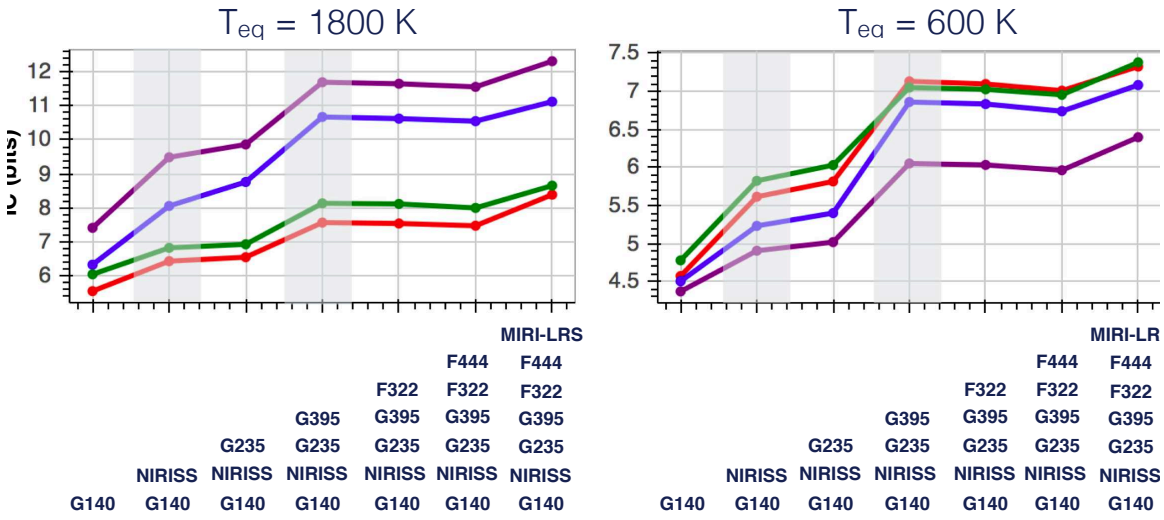

Fig. 6.— Here we show the information content as a function of the addition of an observation mode. The left is the planet system WASP-62b with T_{eq} = 1800 K and on the right is the same but with T_{eq} = 600 K. The lines represent the four combinations of C/O = 1 or 0.55 and Fe/H=1 or 100×Solar. The shaded regions show the highest jumps in information content, which occur with the addition of NIRISS and NIRSpec G395M/H.

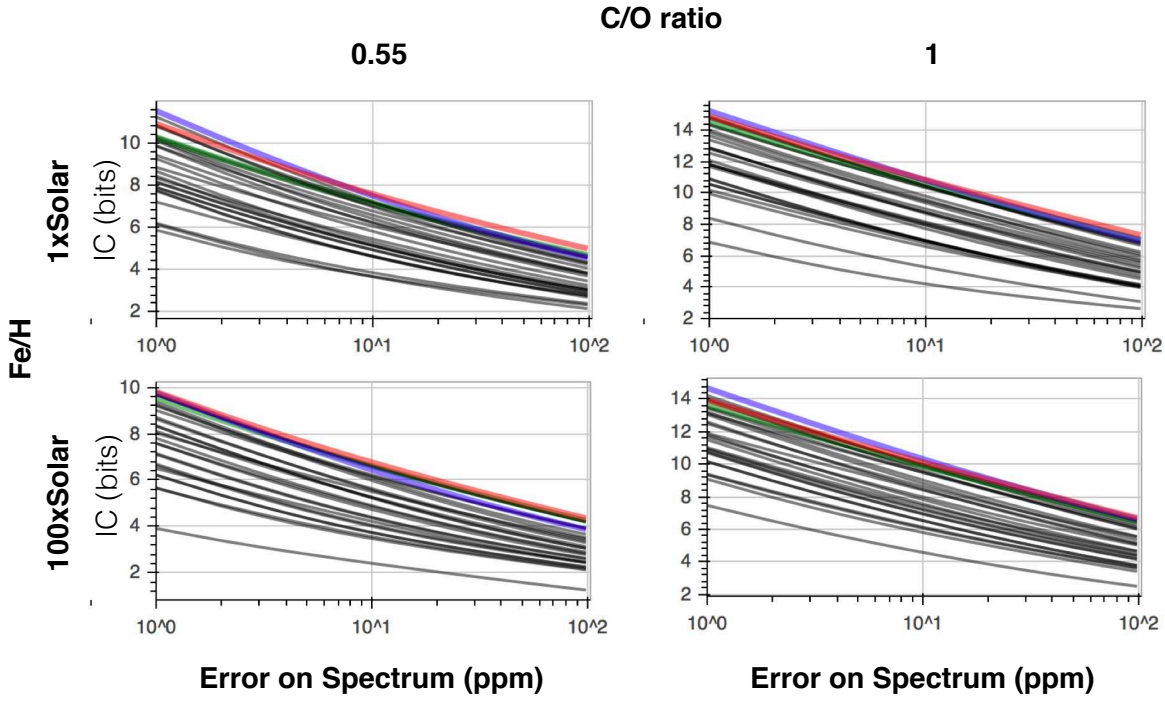

Fig. 7.— Here we show the information content as a function of the addition of error on the planet spectrum. Each line in each panel represents a different combination of modes as shown in Figure 2. The colored lines are the combinations of modes that appear in Table 1, our prediction for the good combination of modes.

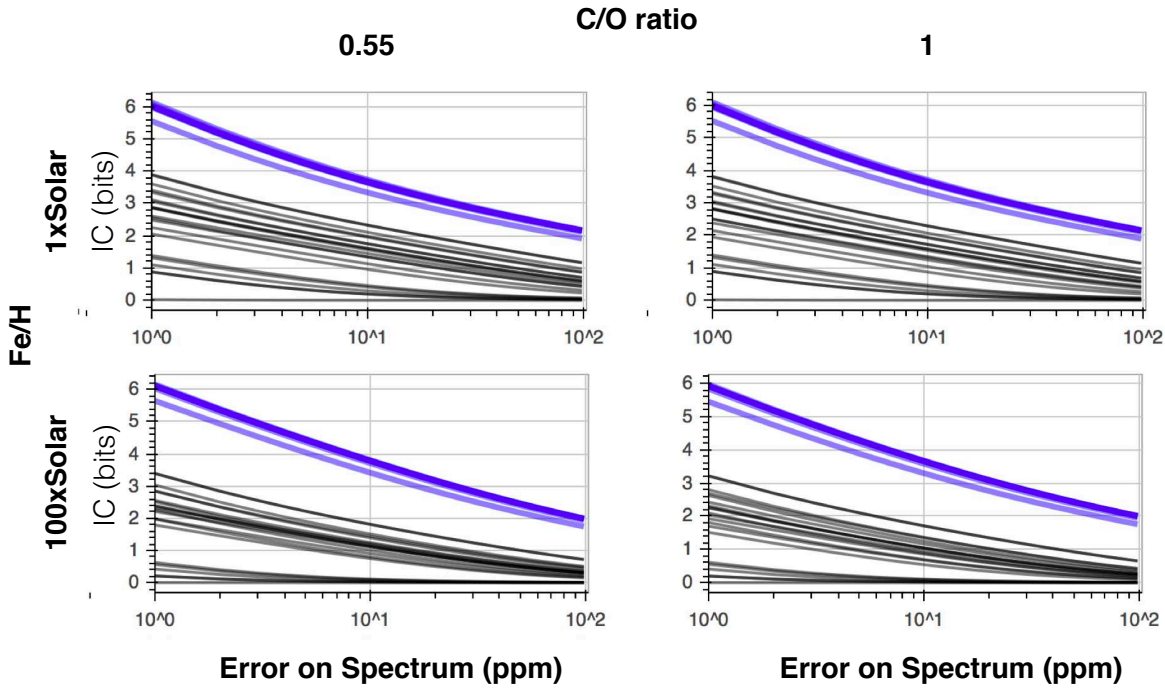

Fig. 8.— Here we show the information content as a function of the addition of error on the planet spectrum. Each line in each panel represents a different combination of modes as shown in Figure 3. The colored lines are the combinations of modes that appear in Table 1, our prediction for the good combination of modes.